MAX-PLANCK-INSTITUT FÜR PLASMAPHYSIK

GARCHING BEI MÜNCHEN

STIMULATED RAMAN SCATTERING FROM PLASMAS IRRADIATED BY NORMALLY AND OBLIQUELY INCIDENT LASER LIGHT

D. Biskamp, H. Welter

IPP 6/129 October, 74

Die nachstehende Arbeit wurde im Rahmen des Vertrages zwischen dem Max-Planck-Institut für Plasmaphysik und der Europäischen Atomgemeinschaft über die Zusammenarbeit auf dem Gebiete der Plasmaphysik durchgeführt.

STIMULATED RAMAN SCATTERING FROM PLASMAS IRRADIATED BY NORMALLY AND OBLIQUELY INCIDENT LASER LIGHT

D. Biskamp, H. Welter

Max-Planck-Institut für Plasmaphysik, Garching, West-Germany

ABSTRACT

The frequency spectrum and the angular distribution of the scattered light, and the absorption coefficient, due to stimulated Raman scattering are obtained by extensive numerical simulations of one and two-dimensional plane plasma targets irradiated normally or obliquely by high-power laser light. Theoretical models are given to explain the numerical results.

Stimulated scattering of light from laser irradiated plasmas has attracted much attention in recent years because of its detrimental influence on the laser-fusion concept. Stimulated Raman scattering (SRS) is due to parametric excitation of an electron plasma wave which coherently scatters off part of the laser intensity. Thresholds and growth rates for SRS have previously been computed for various conditions (see, for instance, Refs. 1,2), and some important nonlinear properties have been found particularly from numerical simulations [1),3)]. The present paper considerably extends previous theoretical understanding.

We first report numerical and theoretical results on the frequency spectrum of the scattered light and the process of dissipation due to SRS. The computed system, one-dimensional in space with transmitting boundary conditions, has a linear density profile with $n_{max} = n_c/2$, an inhomogeneity scale $L \equiv n(dn/dx)^{-1} = 50\ c/\omega_o$ at $n = n_c/4$, and an initial electron temperature $T_{eo}/m_e c^2 = 10^{-3}$. As in all simulations of SRS the ions are assumed immobile. Electrons hitting the boundary on the dense side of the system are absorbed and re-emitted cool to simulate a neat heat flow out of the system and allow a quasi-stationary nonlinear state to be established.

For laser amplitudes $0.06 \lesssim v_o/c \leq 0.1$, $v_o \equiv eE_o/m_e\omega_o$, a plasma wave train is excited localized at $n \simeq n_c/4$ with $\omega = \omega_{pe} = \omega_o/2$. Light absorption is weak in this intensity regime. A remarkable feature is the appearance of a spectrum of anti-Stokes lines in both the transmitted and the reflected light, Fig. 1, with a regular line spacing $\Delta\omega = \omega_{pe}$. The effect can be described by the following model equation, valid for not too large amplitudes,

$$(1) \qquad \frac{\partial^2 A^{(n)}}{\partial t^2} - c^2 \frac{\partial^2 A^{(n)}}{\partial x^2} + \omega_{pe}^2 A^{(n)} = -\omega_{pe}^2 \frac{\tilde{n}}{n} A^{(n-1)} \quad ,$$

where $A^{(n)}$ is the vector potential of the n-th order spectral line. Here $\tilde{n}$ is a finite amplitude plasma wave packet with frequency ω_{pe} and a sufficiently small spatial width, since phase-matching for this process cannot be satisfied exactly in one dimension. For anti-Stokes frequencies in the transmitted light the coupling described by Eq. (1) is efficient (approximate phase-matching) if $\tilde{n}$ has phase velocity along the density gradient, as generated directly by SRS. Production of anti-Stokes lines in the reflected light, however, requires a component of $\tilde{n}$ with phase velocity opposite to the density gradient. This is also found when solving Eq. (1) numerically. Such outbound plasma waves are not excited by the fundamental Raman process,but are generated by reflection of inbound plasma waves at their cut-off slightly above $n_c/4$. The presence of outbound modes is clearly observed in the simulations.

For laser intensities $v_o/c > .1$, strong absorption and electron heating occur, which determines the saturation of the parametric instability, mode-coupling effects such as the production of anti-Stokes lines being weak. A rather turbulent field of electron density oscillations is excited extending beyond $n_c/4$. Electron heating is connected with the formation of a high energy tail in $f_e\ (v_x)$. Although this is a strongly nonlinear effect, the main features of the quasi-stationary state of light reflection and absorption and electron heat conduction may be described by a quasilinear approach, where the frequency and damping rate of the plasma oscillations are determined by the linear dispersion properties due to the distribution f_e including the tail. Since the tail extends beyond the phase velocities of the electrostatic modes excited, the dispersion relation for these modes is changed, containing a new, beam-like branch.

Figure 2 shows frequency, damping rate and phase velocity of this branch for an appropriate model distribution. The frequency is considerably smaller than the plasma frequency, in particular at the point of maximum damping, which permits plasma oscillations to be excited by SRS at $n > n_c/4$. There is also a decrease in phase velocity with increasing strength of the tail. In a self-consistent system this should lead to a reduction of the maximum tail velocity, as is in fact observed in the simulations, see Fig. 3.

Figure 3 also shows the blue shift of the Raman frequency ω_1 due to the reduction of $\omega = \omega_o - \omega_1$, predicted by the modified dispersion relation. Comparing the observed values of ω with the dispersion curves of Fig. 2 where the model distributions have about the same tail population (10% resp. 20%) as the distributions shown in Fig. 3, we find approximate agreement with the values of ω at the point of maximum damping. This is in the spirit of a quasilinear saturation where the modes most strongly driven by SRS require the largest damping rates. The Raman frequency ω_1 and the absorption coefficient A are connected by a relation derived from the Manley-Rowe relations for a three wave parametric process [4]. Introducing the reflection coefficient R and the transmission coefficient T such that $A = 1 - R - T$, it is found that

$$A = \frac{\omega_o - \omega_1}{\omega_o} \quad (1 - T). \tag{2}$$

The values of ω_1 obtained from the frequency spectra und those obtained from Eq. (2) using the observed values of A and T agree quite well, as seen in Table 1. With Eq. (2) the decrease of A with increasing laser intensity in the dissipative regime $v_o/c \gtrsim 0.2$ is related to the reduction of the frequency ω of the electrostatic modes.

The angular distribution of the scattered Raman light is investigated by two-dimensional simulations. Here boundary conditions along the density gradient are identical to those used in the one-dimensional simulations, while we apply periodicity in the transverse direction. A general numerical result is that SRS occurs mainly at those points of the density profile where $k_{1x} \simeq 0$, i.e. at the classical turning points of the scattered light (the localization of SRS at $n_c/4$ in the one-dimensional simulations is a special case of this phenomenon). To explain this behavior, we recall that in an inhomogeneous plasma parametric instabilities are in general convective[5]. Only at particular points may absolute instabilities arise. For SRS it has been shown[6] that the Raman cut-off density $n_c/4$ is such a point. The results of Ref.6 can be generalized to the case of side-scattering ($k_{1y} \neq 0$) and oblique incidence ($k_{oy} \neq 0$). In the limit $\gamma \ll \gamma_o, \gamma_o =$ = homogeneous growth rate, the most interesting case for applications, the wave equation for the vector potential of the scattered wave becomes formally identical with the corresponding equation in Ref. 6,

$$(3)\quad c^2 \frac{d^2 A_1}{d\xi^2} + \left(\frac{L}{\omega_{pe}}\right)^2 \left(\alpha^2 + \frac{V^2 - \gamma^2 - \xi^2}{\xi}\right) A_1 \simeq 0$$

$$\xi = \omega_{pe}^2 \, x/L, \qquad L = n(dn/dx)^{-1}, \qquad V^2 = \omega_{pe}^2 \cos^2\phi \; v_o^2 k^2/4,$$

$$\alpha^2 = \omega_1^2 - k_{1y}^2 c^2 - \omega_{pe}^2, \quad \underline{k} = \underline{k}_o - \underline{k}_1, \quad \underline{A}_o \cdot \underline{A}_1 = A_o A_1 \cos\phi .$$

Thus, in the limit $\gamma \ll \gamma_o$ the various side-scattering processes at $n<n_c/4$ differ from the scattering at $n_c/4$ only by different value of V^2 and $L/\omega_{pe}^2 \propto L/n$, and hence correspond to the same absolute instability. The growth rate increases with increasing V^2 and L/n. As a function of

density and angle of incidence θ_o, we have

$$(4) \quad V^2 \propto (n/n_c)\,(2-2\sqrt{n/nc} - n/n_c - 2k_{oy}\,k_{1y}\,c^2/\omega_o^2)\ ,$$

where $k_{oy}\,c/\omega_o = \sin\theta_o$, and $k_{1y}^2 c^2/\omega_o^2 = 1 - 2\sqrt{n/n_c}$.

To discuss the simulation results in more detail, it is convenient to distinguish between the polarisation vector $\underline{A}_o$ in or perpendicular to the plane of scattering (=plane of incidence for oblique incidence). Let us first consider the latter case. For normal incidence, $k_{oy} = 0$ in Eq. (4), V^2 has a maximum at $n = n_c/4$, but only slowly decreases with decreasing n. Thus, for a linear density profile, L/n = const, there should be back-scattering at $n_c/4$ and side-scattering at some lower density, with back-scattering slightly dominating. This is, in fact, observed in the simulations see Fig. 4 (note that side-scattering leads to scattered light outside the plasma propagating at some angle θ_1 because of refraction, $\tan\theta_1 = k_{1y}/k_{1x} = \left[(1-2\sqrt{n/n_c})\,n_c/n\right]^{1/2}$). For an exponential density slope, L = const, however, scattering at some $n < n_c/4$ dominates because of the larger L/n.

For oblique incidence simulations show that SRS always takes place at some $n < n_c/4$. Side-scattering with $k_{oy}\,k_{1y} < 0$ dominates, thus leading to Raman light propagating back into the quadrant of incidence. The results can be explained by the theory outlined above. Given a density profile and an angle of incidence θ_o, the scattering mode with the largest growth rate can be computed in a straightforward way, e.g. for a linear profile and $\theta_o = 23^o$, $\gamma_{max} = \gamma\ \{n=.2n_c\} \simeq 1.24\gamma\ \{n=n_c/4\}$. Thus in general the frequency ω_1 of the Raman light is higher than $\omega_o/2$, and SRS at $n_c/4$ as seen in the one-dimensional simulations is found only under rather special conditions. The conclusions from those simulations, however, i.e. the

generation of Raman anti-Stokes light and the process of the dissipation, are valid, if suitably modified, also in higher dimensions.

For polarization vector in the plane of scattering SRS is found to be much weaker, owing to $V^2 \propto \cos^2\phi$ and to the presence of the $2\omega_{pe}$ decay instability. For oblique incidence this is the dominating process taking place at $n \simeq n_c/4$ irrespective of the angle of incidence and leading to considerable absorption of laser light. Some light ($\lesssim 5\%$) may also be anomalously scattered off the plasma oscillations due to $2\omega_{pe}$-decay. The scattering is mainly specular with frequencies at ω_o and $3\,\omega_o/2$, and a very small contribution at $\omega_o/2$. Thus the rather narrow lines at $\omega_o/2$ and $3\omega_o/2$, with the latter strongly dominating, recently observed experimentally [7)8)], are probably due to the $2\omega_{pe}$-decay and not to SRS. The absence of SRS in those experiments is explained by the relatively high threshold which is usually above the threshold for $2\omega_{pe}$-decay.

In conclusion, we have presented simulation and theoretical results on stimulated Raman scattering in an inhomogeneous plasma concerning the frequency spectrum of the scattered light, the process of absorption, and the angular distribution of scattered light for general direction of incidence of the laser light. For polarisation in the plane of incidence the $2\omega_{pe}$-decay is stronger than SRS and seems to be responsible for the half harmonic frequencies, essentially $3\omega_o/2$, recently observed experimentally.

"This work was performed under the terms of the agreement on association between the Max-Planck-Institut für Plasmaphysik and EURATOM".

REFERENCES

1) D.W. Forslund, J.M. Kindel, and E.L. Lindman,
Phys. Rev. Lett. 30, 739 (1973)

2) A.A. Galeev, G. Laval, T.M. O'Neil, M.N. Rosenbluth, and R.Z. Sagdeev,
Sov. Phys. JETP Lett. 17, 48 (1973)

3) H.H. Klein, W.M. Manheimer, and E. Ott, Phys. Rev. Lett. 31, 1187 (1973)

4) W.H. Louisell, Coupled Mode and Parametric Electronics, John Wiley & Sons,
Inc., New York-London, 1960

5) M.N. Rosenbluth, Phys. Rev.Lett. 29, 565 (1972)

6) J.F. Drake and Y.C. Lee, Phys. Rev. Lett. 31, 1197 (1973)

7) J.L. Bobin, M. Decroisette, B. Meyer and Y. Vitel
Phys. Rev. Lett. 30, 594 (1973)

8) Ping Lee, D.V. Giovanelli, R.P. Godwin, G.H. McCall
Appl. Phys. Lett. 24, 406 (1974)

FIGURE AND TABLE CAPTIONS

Fig. 1 Frequency spectrum of the reflected and the transmitted light, $R(\omega)$ and $T(\omega)$, plotted on a logarithmic scale, for nondissipative SRS, from a one-dimensional simulation with $v_o/c = 0.1$.

Fig. 2 Solution of the dispersion relation for a model distribution f_e, consisting of a bulk (=δ-function at $v = 0$) and a linearily decreasing tail, containing 10%, upper diagram, and 20%, lower diagram, of the electrons. Velocity and frequency are normalized to the maximum tail velocity and the total plasma frequency. For large k ω approaches the plasma frequency of the bulk density.

Fig. 3 Frequency spectra of the reflected light $R(\omega)$ and distribution functions $f_e(p_x)$ for dissipative SRS, from two one-dimensional simulations, $v_o/c = 0.2$ upper row, $v_o/c = 0.3$ lower row.

Fig. 4 Plots of simulation electrons from two-dimensional runs with normal incidence, $v_o/c = 0.1$

a) linear density profile $n(x) = (0.2x/48 + 0.1)n_c$

b) exponential profile $n(x) = 0.3 \exp\{(x-48)/50\}$

TABLE 1. Reflectivity R, transmission coefficient T, absorption coefficient A, and frequency of the plasma modes ω for two runs, $v_o/c = 0.2$ and 0.3. $\omega/\omega_o/_{theor}$ is obtained from Eq. (2), $\omega/\omega_o/_{exp}$ by measuring $\omega_o - \omega_1$ in the frequency spectrum of the reflected light.

v_o/c	R	T	A	ω/ω_o /theor.	ω/ω_o /exp.
0.2	0.43	0.27	0.30	0.40	0.41
0.3	0.41	0.43	0.16	0.28	0.30

TABLE 1

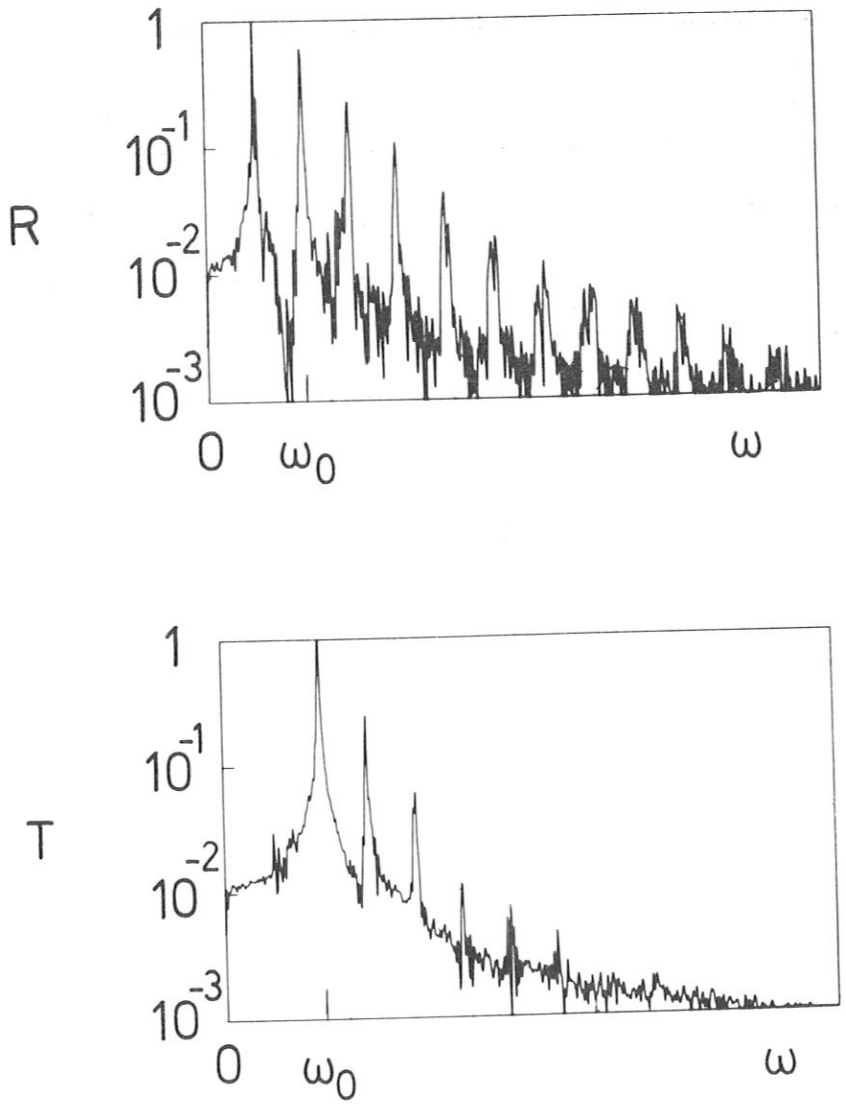

Fig.1

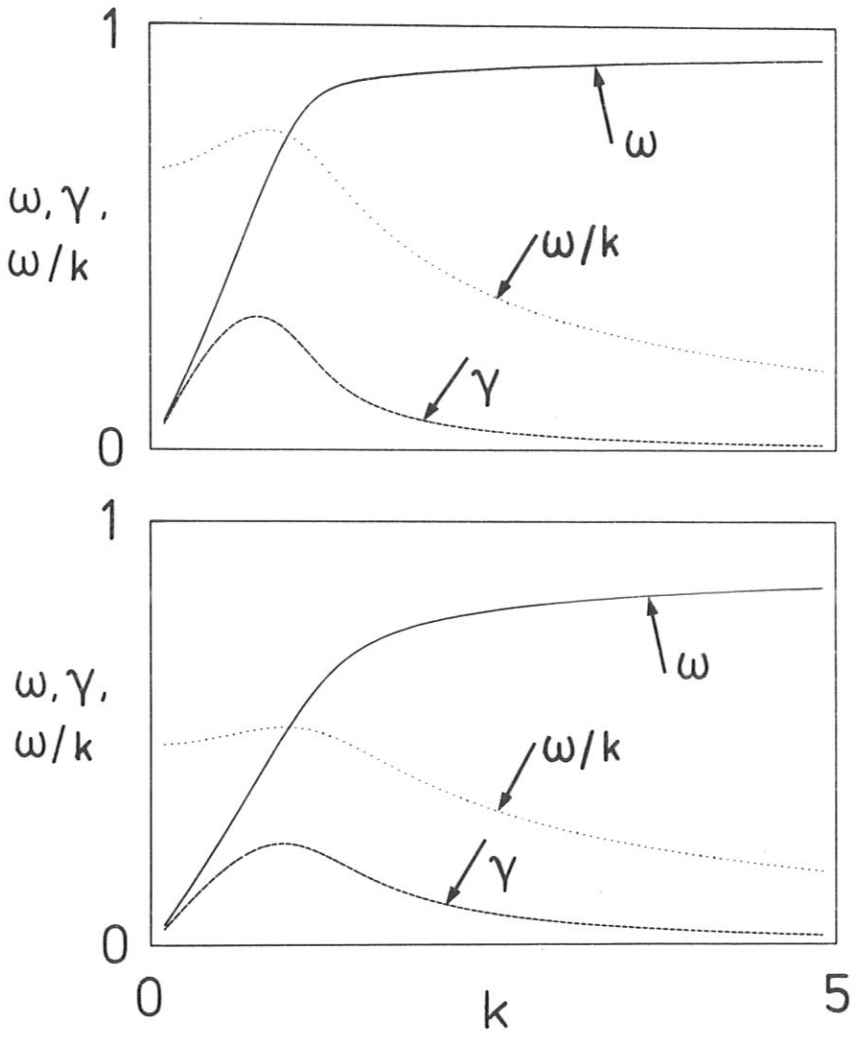

Fig. 2

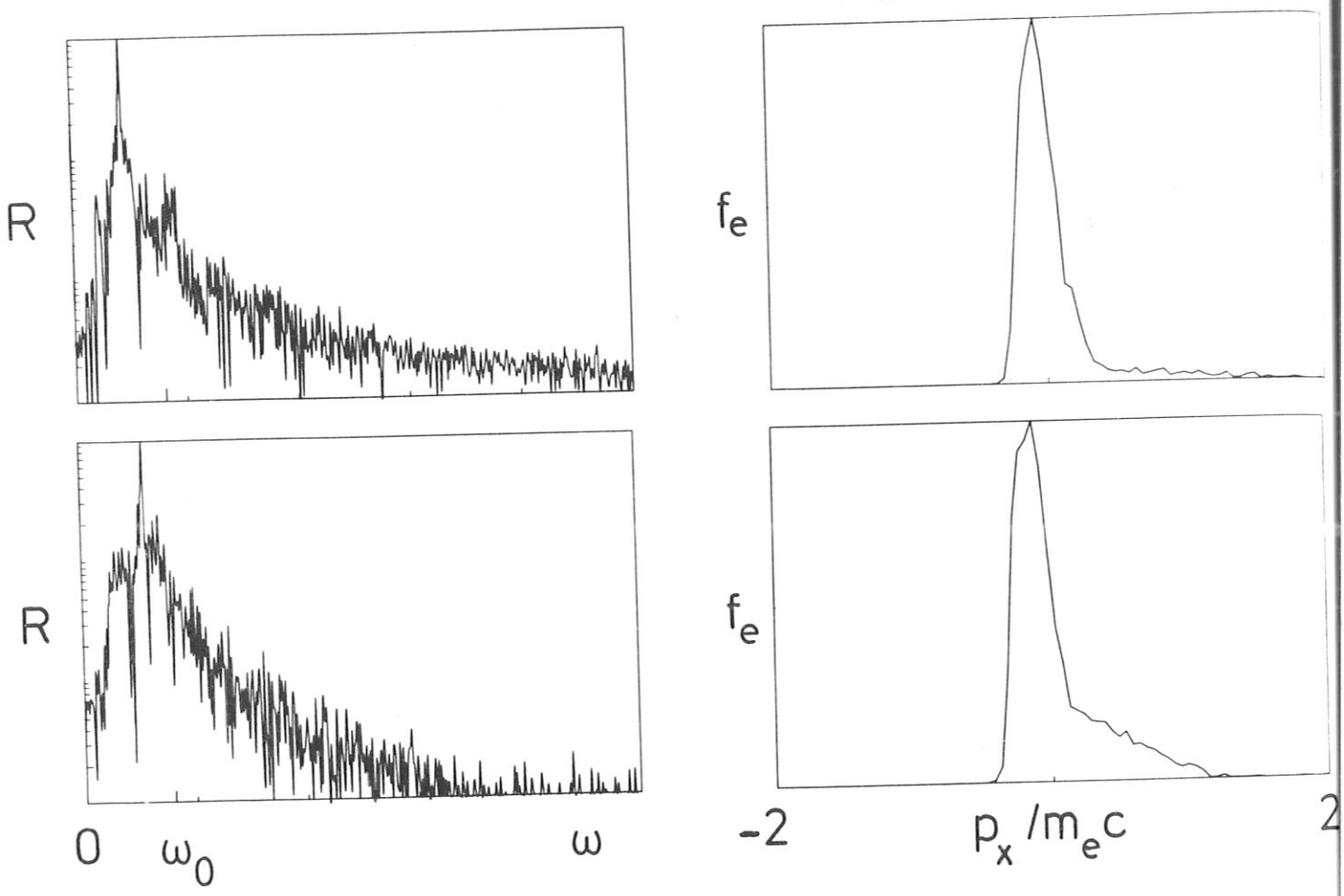

Fig. 3

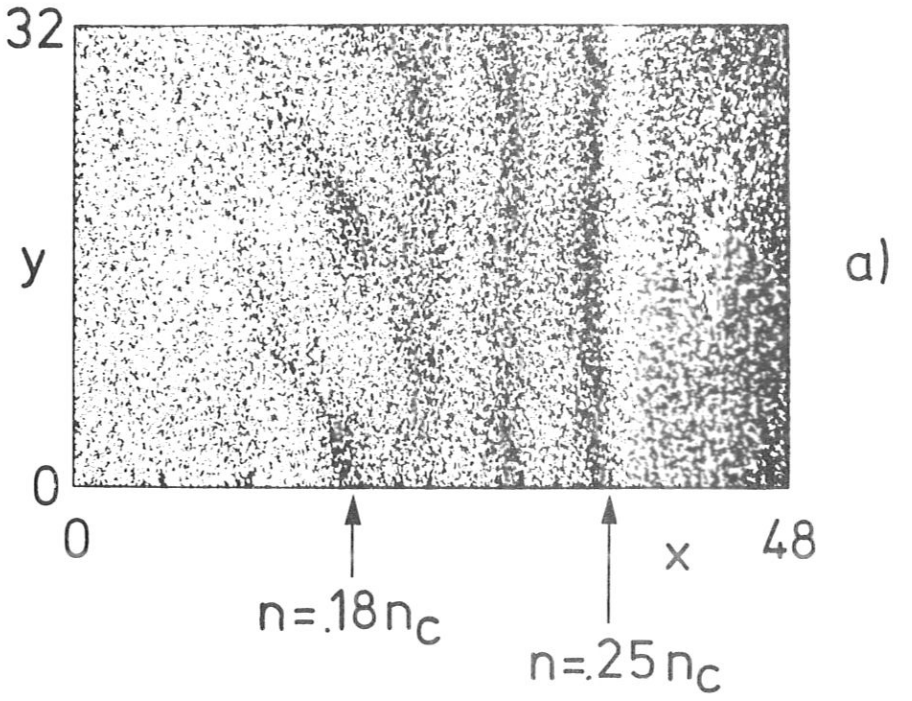

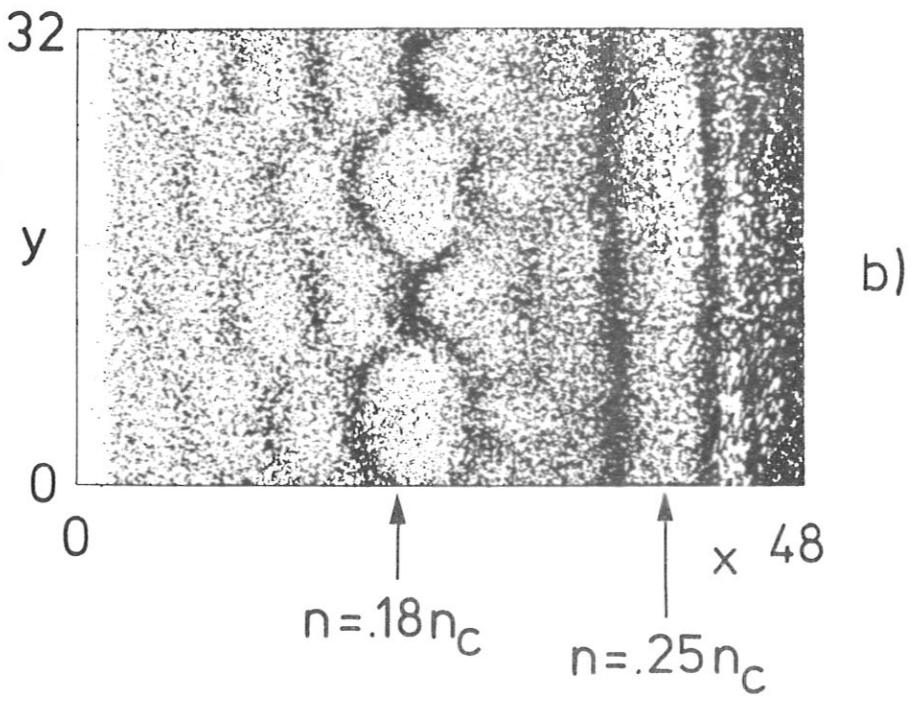

Fig. 4